ELSEVIER

Journal of Alloys and Compounds 323–324 (2001) 731–735

Journal of ALLOYS AND COMPOUNDS

www.elsevier.com/locate/jallcom

Room temperature photon avalanche in Ho^{3+} doped YAG, YAP, YLF and ZBLAN

M. Malinowski[a,*], A. Wnuk[a], Z. Frukacz[b], G. Chadeyron[c], R. Mahiou[c], S. Guy[d], M.F. Joubert[d]

[a]*Institute of Microelectronics and Optoelectronics PW, ul. Koszykowa 75, 00-662 Warsaw, Poland*
[b]*Institute of Electronic Materials Technology, ul. Wólczynska 133, 01-919 Warsaw, Poland*
[c]*Laboratoire des Materiaux Inorganiques, ESA-6002, Universite Blaise Pascal and ENSCCF, F-63177 Aubiere Cedex, France*
[d]*Laboratoire de Physico-Chimie des Materiaux Luminescents, UMR 5620 du CNRS, Universite Lyon 1, Bat. 205, 69622 Villeurbanne, France*

Abstract

Upconverted, green emission from the $^5S_2$ level of Ho^{3+} ion in two oxides, YAG and YAP, and two fluorides, YLF and ZBLAN, was observed at room temperature under cw 580–590 nm excitation. Under these excitation wavelengths, which are off resonance with any ground state absorption, characteristic features of photon avalanche process are observed. A time-dependent rate equation model was employed to describe this behavior using experimentally determined parameters. © 2001 Published by Elsevier Science B.V.

Keywords: Photon avalanche; Upconversion; Holmium ion; Energy transfer; Nonlinear processes

1. Introduction

Applications in optical data storage, full color displays and medical instrumentation have stimulated the development of lasers working in the visible spectral range. One possible way of creating visible emitting laser pumped by readily available, semiconductor infrared or red laser diode is to exploit multi-photon processes. Generally, an upconversion laser produces laser light at a shorter wavelength than the pump light [1,2]. Thus, the processes of conversion of infra-red (IR) or visible radiation into shorter wavelength visible radiation are being currently studied in various systems containing rare-earth (RE) or transition metal ions.

Among several upconversion mechanisms, photon avalanche is one of the most efficient and complicated, it combines two processes: excited state absorption (ESA) and cross relaxation [3,4]. In avalanche excitation the pump light is resonant with a transition between two excited states and off-resonance with ground state absorption. Above threshold pumping intensity, the system becomes absorptive and upconversion emission occurs [5,6]. Thus, interest in understanding and modeling avalanche process is necessary both for a fundamental point of view and for potential applications in upconversion lasers and bistable optical devices. Whereas in Sm^{3+} or Nd^{3+}-doped hosts in which photon avalanche was observed only at low temperatures (<100 K), room temperature photon avalanche occurs in Pr^{3+}, Tm^{3+}, Er^{3+}-doped or $Yb^{3+}+Pr^{3+}$-doped materials (see [7] for a review) and room temperature photon avalanche pumped upconversion lasers were demonstrated with $Yb^{3+}+Pr^{3+}$-doped YLF crystal [8] and ZBLAN fiber [9,10].

The present study focuses on avalanche upconversion excitation of higher lying states of Ho^{3+} ion in two types of systems; oxide crystals of YAP and YAG and also fluoride hosts; crystal of YLF and ZBLAN glass. Trivalent holmium ion (Ho^{3+}) has several metastable levels which offer multiple possibility of laser transitions at various wavelengths from the ultra-violet region to IR [11]. Several holmium activated crystals have been made to lase in the green part of the spectrum, between transitions from the excited $^5S_2$ manifold to the ground state as the result of one-photon high-energy excitation [12,13]. Also, recently green Ho^{3+}-doped fluorozirconate glass (ZBLAN) fiber upconversion laser was demonstrated [14–16]. First observation of Ho^{3+} avalanche upconversion in ZBLAN was reported in [17] and in [18,19] we have presented results of an avalanche absorption in YAP crystals.

In this work we report, on the avalanche upconversion in holmium-doped YAG and YLF crystals. Steady state emission, temporal evolution near the threshold and the

*Corresponding author. Tel.: +48-22-660-7783; fax: +48-22-628-8740.

E-mail address: m.malinowski@imio.pw.edu.pl (M. Malinowski).

0925-8388/01/$ – see front matter
PII: S0925-8388(01)01064-7

excitation power dependence of the green fluorescence are analyzed in the four studied YAG, YAP, YLF and ZBLAN hosts using a three-level rate equation model.

2. Experimental results and discussion

The samples used were a bulk ZBLAN glass doped with 1% of HoF_3, a $LiYF_4$ (YLF) crystal doped with 1at.% Ho^{3+} and $Y_3Al_5O_{12}$ (YAG) and $YAlO_3$ (YAP) crystals doped with holmium (several concentrations from 0.1 to 5 at.%). All experiments were performed at 300 K, with a cw dye laser as the excitation source; the details of the experimental apparatus used in our studies have been described previously [18].

Strong, upconverted green fluorescence corresponding to the $^5S_2 \rightarrow {}^5I_8$ transition of Ho^{3+} ions was generated in all investigated samples by the cw orange light excitation in the 580–590 nm spectral range. This upconversion has the main distinctive features of the avalanche process such as the existence of a pump threshold, the concave shape of the temporal dependence of the upconversion fluorescence intensity and the critical slowing down of the transient signals at the threshold [6].

Absorption and avalanche excitation spectra of Ho^{3+}:YLF crystal, presented in Fig. 1, indicate that there is no resonant transition from the ground state when pumping at about 580 nm. From the energy level diagram of Ho^{3+} ion it results that excitation energy is about 1500 cm^{-1} above the $^5F_5$ state and that the observed excitation wavelengths correspond to the two $^5I_7 \rightarrow {}^5G_6$ and $^5I_7 \rightarrow {}^5F_1$ ESA transitions. The $^5I_7$ long-lived metastable state acts as good population reservoir and allows a high density of excited ions to be created. The laser being tuned to these $^5I_7 \rightarrow {}^5G_6 + {}^5F_1$ ESA transitions, we observed strong transitions from all Stark components of $^5I_7$ to the three $^5F_1$ Stark levels and much less intense transitions terminating in the highest component of the $^5G_6$ manifold. Then, fast nonradiative relaxation occurs to the $^5S_2$ manifold [18]. So, the essential Ho^{3+} levels which take part in the process are the $^5I_8$ ground state, the $^5I_7$ metastable state and the $^5S_2$ green emitting level. The diagram of the proposed avalanche mechanism is shown in Fig. 2.

Measurements of green fluorescence intensity versus incident orange laser power were made and results are illustrated in Fig. 3. For YAP, YLF and ZBLAN this green emission increases suddenly of more than one order of magnitude with a slope much higher than 2 on a logarithmic plot, under excitations power of about 110, 170 and 100 mW, respectively. This is due to creation of additional population in level 2 by avalanche mechanism and correspond to the typical photon avalanche threshold. Fig. 4 shows the time dependence of the $^5S_2 \rightarrow {}^5I_8$ upconverted fluorescence for different excitation powers in the case of YLF:1% Ho^{3+}. The time of establishment τ_c, defined as the time necessary to reach 95% of the stationary intensity, is maximum at the threshold power; it is much longer than the $^5I_7$ metastable state lifetime of 17 ms. When the excitation power exceeds the threshold value, a 'concave up' shape appears in the transient curves and τ_c becomes shorter. This time behavior as well as the stationary intensity values versus the incident excitation power are presented together in Fig. 5. For YAG:Ho^{3+} the threshold behavior is not clearly observed in Fig. 4, however it can be distinguished from the time-dependent measurements (see Fig. 6).

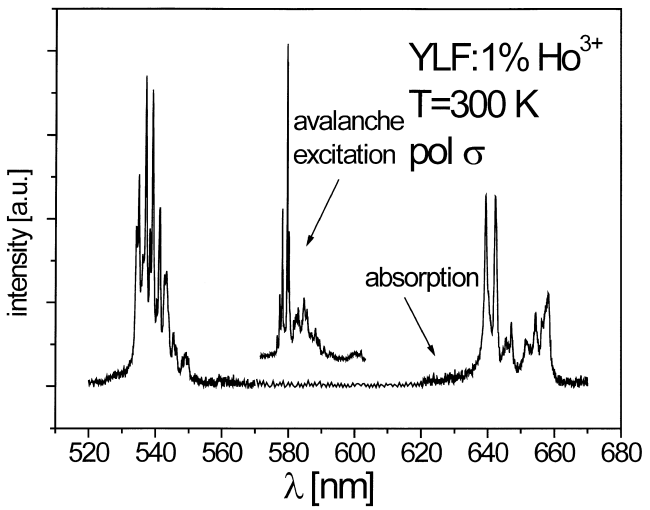

Fig. 1. 300 K absorption and avalanche upconversion excitation spectra of YLF:1% Ho^{3+} in the yellow–orange excitation region. Upconversion excitation spectra were recorded with detection of the $^5S_2 \rightarrow {}^5I_8$ green luminescence.

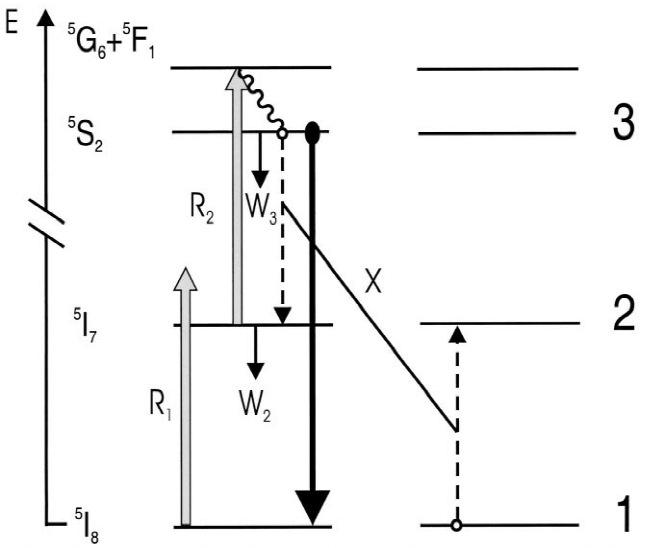

Fig. 2. Energy level diagram of Ho^{3+} used in modeling the avalanche upconversion process.

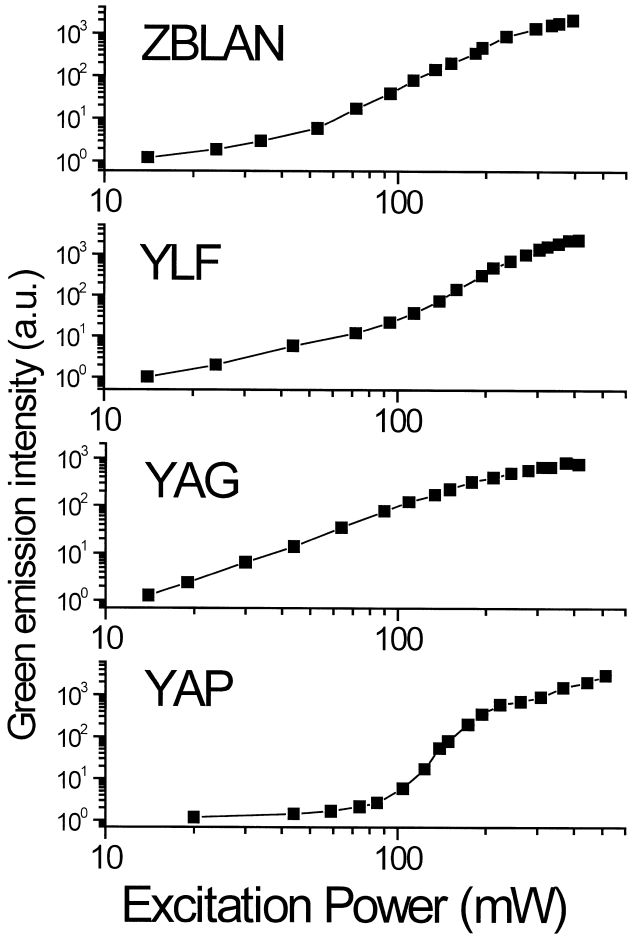

Fig. 3. Double logarithmic plot of the power dependence of the $^5S_2 \rightarrow {}^5I_8$ upconversion luminescence in the investigated holmium-activated materials measured at 300 K.

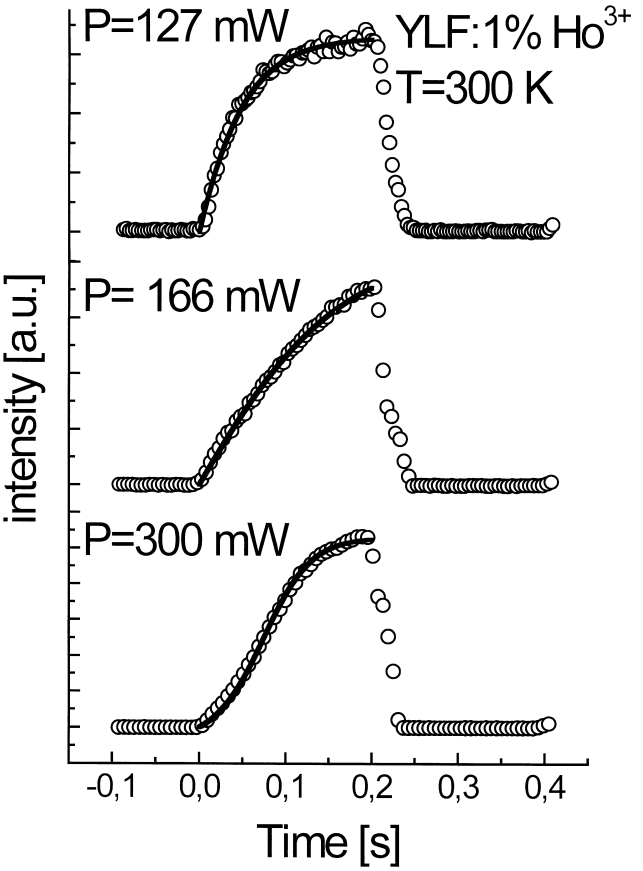

Fig. 4. Temporal behavior of the upconverted $^5S_2 \rightarrow {}^5I_8$ fluorescence in YLF:1% Ho^{3+} for different excitation powers at 579.6 nm. Open circles represent experimental points and the solid line is the result of the numerical analysis.

3. Theoretical model

The following rate equation system is used to describe the dynamical behavior of the populations of the $^5I_8$, $^5I_7$ and $^5S_2$ energy levels (Fig. 2) and its solution in the long-time limit gives insight into the stationary fluorescence intensity dependence on pump power.

$$n_1 = -R_1 n_1 + W_2 n_2 + \beta W_3 n_3 - X n_1 n_3$$

$$n_2 = R_1 n_1 - (W_2 + R_2) n_2 + (1-\beta) W_3 n_3 + 2X n_1 n_3$$

$$n_3 = R_2 n_2 - W_3 n_3 - X n_1 n_3$$

$$1 = n_1 + n_2 + n_3$$

In this system, n_i denotes the population in level i, X is the cross relaxation energy transfer rate that couples two Ho^{3+} ions, R_1 and R_2 ($R_i = I\sigma_i/h\nu$) are the ground and excited state pumping rates, respectively, β is the branch-

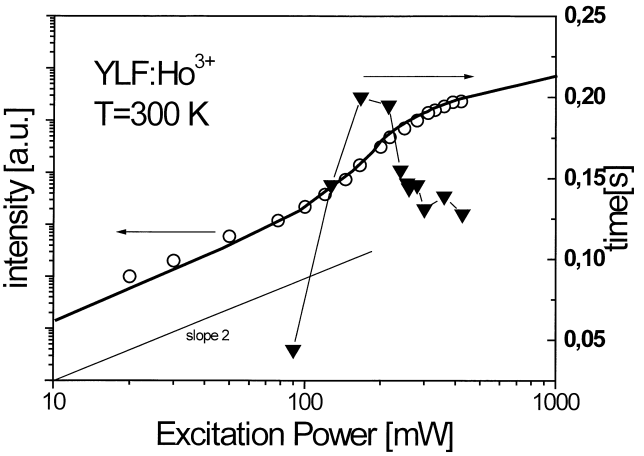

Fig. 5. Double logarithmic plot of the power dependence and time establishment of the $^5S_2 \rightarrow {}^5I_8$ upconversion luminescence in YLF:1% Ho^{3+} at 300 K. Open circles represent experimental points and the solid line is the result of the numerical analysis.

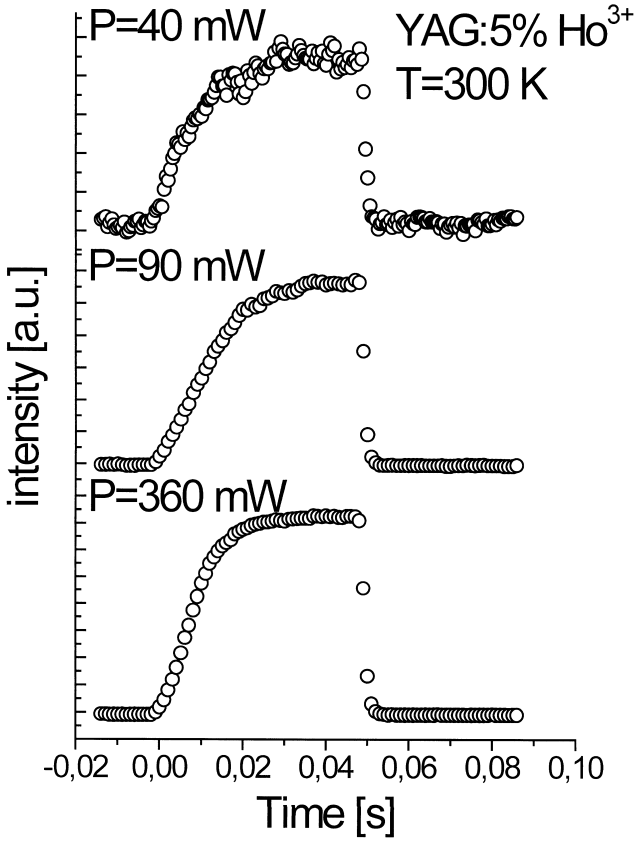

Fig. 6. Temporal behavior of the upconverted $^5S_2 \rightarrow {}^5I_8$ fluorescence in YAG:5% Ho^{3+} for different excitation powers at 594 nm.

ing ratio representing the fraction of n_3 population that decays to level 1. W_2 and W_3 are the relaxation rates of levels 2 and 3 (in the low concentration limit), respectively.

The excited state absorption cross-sections and the radiative relaxation rates were calculated using Judd–Ofelt [20,21] formalism. Experimental green fluorescence decays permitted to estimate the non radiative multiphonon as well as cross relaxation energy transfer rates. β is estimated taking into account the calculated radiative branching ratios and the multiphonon relaxation rate from level 3. Then, the numerical solutions have been compared with 300 K experimental data in both steady state and transient regimes. The only fitted parameter was the value of the cross section ratio σ_2/σ_1.

A summary of the spectroscopic parameters of the investigated materials which characterize the avalanche process and which were used in theoretical modeling are given in Table 1. In Figs. 4 and 5 the best fit curves (solid line) are superimposed on the experimental data. Modeling of the avalanche excitation process using this rate equation analysis was successful in the case of holmium-doped YAP, YLF and ZBLAN. For YAG, there is no satisfactory agreement between experiment and theory, this is why we did not write any σ_2/σ_1 parameter in Table 1. The main difference for this material is that the $^5S_2$ fluorescence lifetime is only 4.5 μs which is much shorter than in most, including oxides, holmium-activated materials [22], suggesting its predominantly nonradiative character. This is probably the reason why a drastic increase of photon avalanche upconverted green fluorescence cannot be observed in this crystal.

4. Conclusions

We have observed avalanche upconversion in several holmium-doped matrix when pumping in the 580–590 nm spectral range. Both, the power dependence and dynamic behavior have been analyzed with a rate equation model. The agreement between the experiment and the model was obtained for Ho-doped YAP, ZBLAN and YLF. In the case of Ho-doped YAG, the photon avalanche effect is screened by very efficient multi-phonon relaxation which quenches the green emission.

Table 1
Spectroscopic parameters which characterize the avalanche upconversion process in the investigated Ho^{3+} materials

	YAG:5% Ho	YAP:5% Ho	YLF:1% Ho	ZBLAN:1% Ho
P_{th} [mW]	90	110	164	124
I_{th} [kW/cm^2]	12.9	15.5	23.4	17.7
λ_{exc} [nm]	594	586	580	581
σ_2 [10^{-20} cm^2]	4.7	0.98	0.03	0.11
Judd–Ofelt calc.				
σ_2/σ_1	22	100	100	33
X [ms^{-1}]	170	98	5.83	3.12
τ_c [s]	0.025	0.054	0.21	0.3
τ_2 [ms]	6.6	8.6	17	12
τ_3 [ms]	0.0045	0.058	0.13	0.34
at low concentration				
$W_2 = 1/\tau_2$ [ms^{-1}]	0.152	0.116	0.059	0.083
$W_3 = 1/\tau_3$ [ms^{-1}]	222	17.24	7.62	2.94
at low concentration			[23]	[24]
β ($^5S_2 \rightarrow {}^5I_8$)	0.01	0.13	0.02	0.04

Acknowledgements

This work was supported by the Polish State Committee on Science (KBN) — project no. 8 T11B 08117 — and Polish–French program 'Polonium' — project no.99046.

References

[1] A.J. Silversmith, W. Lenth, R.M. Macfarlane, Appl. Phys. Lett. 51 (1987) 1977.
[2] P. Xie, T.R. Gosnell, Opt. Lett. 20 (1995) 1014.
[3] J. Chivian, W. Case, D. Eden, Appl. Phys. Lett. 35 (1979) 124.
[4] W. Lenth, R.M. Macfarlane, J. Lumin. 45 (1990) 346.
[5] M.F. Joubert, S. Guy, B. Jacquier, Phys. Rev. B 48 (1993) 10031.
[6] S. Guy, M.F. Joubert, B. Jacquier, Phys. Rev. B 55 (1997) 8240.
[7] M.F. Joubert, Opt. Mater. 11 (1999) 181.
[8] T. Sandrock, E. Heumann, G. Huber, B.T. Chai, in: S.A. Payne, C. Pollack (Eds.), OSA Proceedings on Advanced Solid State Lasers, Vol. 1, Optical Society of America, Washington, DC, 1996, p. 550.
[9] P. Xie, T.R. Gosnell, Opt. Lett. 20 (1995) 1014.
[10] H. Scheife, T. Sandrock, E. Heumann, G. Huber, C. Pollock, W. Bosenberg (Eds.), OSA TOPS Advanced Solid State Lasers, Vol. 10, Optical Society of America, Washington, DC, 1997.
[11] G.H. Dieke, H.M. Crosswhite, Appl. Opt. 2 (1963) 675.
[12] A.A. Kaminskii, V.M. Garmosh, G.A. Ermakov, V.A. Akkerman, A.A. Filmonov, K. Kurbarov, Izv. Akad. Nauk SSSR, Ser. Neorg. Mater. 22 (1986) 1576.
[13] I.G. Podkolzina, A.M. Tkaczuk, V.A. Fedorov, P.P. Feofilov, Opt. Spektrosk. 40 (1976) 196.
[14] J.Y. Allain, M. Monerie, H. Poignant, Electronics Lett. 26 (1990) 261.
[15] D.S. Funk, S.B. Stevens, S.S. Wu, J. Gary Eden, IEEE J.Quantum Electron. 32 (1996) 638.
[16] D.S. Funk, J.G. Eden, IEEE J. Sel. Top.Quantum Electron. 1 (1995) 784.
[17] G.K. Liu, Y.H. Chen, J.V. Beitz, J. Lumin. 81 (1999) 7.
[18] M. Malinowski, R. Piramidowicz, Z. Frukacz, G. Chadeyron, R. Mahiou, M.F. Joubert, Opt. Mater. 12 (1999) 409.
[19] M.F. Joubert, S. Guy, M. Malinowski, R. Piramidowicz, A. Wnuk, G. Chadeyron, Radiation Eff. Def. Solids 150 (1999) 79.
[20] B.R. Judd, Phys. Rev. 127 (1962) 750.
[21] G.S. Ofelt, J. Chem. Phys. 37 (1962) 511.
[22] M. Malinowski, Z. Frukacz, M. Szuflinska, A. Wnuk, M. Kaczkan, J. Alloys Comp. 300–301 (2000) 389.
[23] L. Gomes, L.C. Courrol, L.V.G. Tarelho, I.M. Ranieri, Phys. Rev. B 54 (1996) 3825.
[24] K. Tanimura, M.D. Shinn, W.A. Sibley, M.G. Drexhage, R.N. Brown, Phys. Rev. B 30 (1984) 2429.